Key Points:
- The continental energy storage from 1950–2000 is assessed in simulations from 32 CMIP5 models
- All CMIP5 simulations underestimate the continental heat storage relative to estimates from observed geothermal data
- The shallow subsurface depth of CMIP5 land surface models falsely limits subsurface heat storage and thermal memory

First assessment of continental energy storage in CMIP5 simulations

Francisco José Cuesta-Valero[1], Almudena García-García[1], Hugo Beltrami[1,2], and Jason E. Smerdon[3]

[1]Climate and Atmospheric Sciences Institute and Department of Earth Sciences, St. Francis Xavier University, Antigonish, Nova Scotia, Canada, [2]Centre ESCER pour l'étude et la simulation du climat à l'échelle régionale, Université du Québec à Montréal, Montreal, Quebec, Canada, [3]Lamont-Doherty Earth Observatory, Columbia University, Palisades, New York, USA

Abstract Although much of the energy gained by the climate system over the last century has been stored in the oceans, continental energy storage remains important to estimate the Earth's energy imbalance and also because crucial positive climate feedback processes such as soil carbon and permafrost stability depend on continental energy storage. Here for the first time, 32 general circulation model simulations from the fifth phase of the Coupled Model Intercomparison Project (CMIP5) are examined to assess their ability to characterize the continental energy storage. Results display a consistently lower magnitude of continental energy storage in CMIP5 simulations than the estimates from geothermal data. A large range in heat storage is present across the model ensemble, which is largely explained by the substantial differences in the bottom boundary depths used in each land surface component.

1. Introduction

The ocean heat storage component of the Earth's energy budget for the second half of the 20th century is about $14 \pm 2 \times 10^{22}$ J [*Levitus et al.*, 2005, 2009], while the continental subsurface stored $8 \pm 1 \times 10^{21}$ J during the same period [*Beltrami*, 2002; *Beltrami et al.*, 2002; *Huang*, 2006]. Although the magnitude of the continental heat storage is smaller than the uncertainty range of the estimated ocean heat storage component, the heat storage in the continental subsurface is important for determining the distribution of the Earth's energy budget and the magnitude of the Earth's energy imbalance [*Hansen et al.*, 2011]. Additionally, several climate processes with potentially important climate feedback mechanisms take place in the shallow subsurface and their stability and evolution are dependent on the long-term thermal state of the ground. Processes such as the stability of the soil carbon pool [*Friedlingstein et al.*, 2006; *Sitch et al.*, 2008; *Arora et al.*, 2013; *Hicks Pries et al.*, 2016] and the stability of large areas of permafrost [*Tarnocai et al.*, 2009; *Koven et al.*, 2013; *Slater and Lawrence*, 2013] require robust estimates of continental energy fluxes for proper long-term modeling of their conditions in a future climate.

Because the energy contribution from the Earth's interior to the storage of energy in the continental subsurface can be considered constant on timescales of millions of years or less, changes in the storage of continental heat [*Beltrami*, 2002; *Beltrami et al.*, 2002; *Huang*, 2006] due to climate fluctuations are determined by the physics of the energy exchanges at the air-ground interface, that is, the coupling of the lower atmosphere and the subsurface [*Stieglitz and Smerdon*, 2007; *González-Rouco et al.*, 2009] including the subsurface thermal properties that control heat diffusion underground [e.g., *Pollack et al.*, 2005]. In a coupled general circulation model (GCM), the magnitude of the subsurface heat storage also depends on the depth of the bottom boundary, and a land surface component with a shallow bottom boundary limits the accumulation of heat in the subsurface [*Stevens et al.*, 2007; *MacDougall et al.*, 2010]. For instance, the effect of a shallow bottom boundary on the magnitude of subsurface heat storage has been shown to be more important than the effects of different emission scenarios in a GCM simulation of 21st century climate projections [*MacDougall et al.*, 2008; *González-Rouco et al.*, 2009]. Additionally, deeper land surface components can simulate the soil thermal regimes more realistically, improving the representation of ground surface processes such as permafrost dynamics [*Smerdon and Stieglitz*, 2006; *Alexeev et al.*, 2007; *Lawrence et al.*, 2008; *Nicolsky et al.*, 2007]. Land surface components usually prescribe zero-flux constraints as a bottom boundary condition for climate simulations, which is an unrealistic flux condition [e.g., *Oleson et al.*, 2010; *Roeckner et al.*, 2003; *Dunne et al.*, 2012] that can affect the simulated ground thermal regime [*Weidong et al.*, 2002] altering related ground

temperature processes, such as ground hydrology [*Krakauer et al.*, 2013], the simulation of basal temperatures for ice sheets [*Pollard et al.*, 2005], permafrost evolution [*Oelke and Zhang*, 2004], and soil respiration [*Hicks Pries et al.*, 2016].

Here we use simulations from 32 GCMs from the fifth phase of the Coupled Model Intercomparison Project (CMIP5) [*Taylor et al.*, 2011] to carry out the first assessment of heat storage in the continental subsurface as simulated by CMIP5 models. The simulated estimates are compared to observational estimates derived from the global database of terrestrial borehole temperature measurements. We additionally evaluate the extent of heat storage in the CMIP5 models assuming surface temperatures that are propagated into a continental subsurface extending to a depth of 500 m, as opposed to the much shallower depths in the actual land components of the GCMs (less than 50 m). Our analysis demonstrates the importance of the bottom boundary depth in the context of continental energy storage in GCM simulations and further provides a framework for understanding possible sources of variability in the simulation of subsurface energy content.

2. Data and Methodology

2.1. Model Data

We use the first ensemble member from the Historical simulations and multiple Representative Concentration Pathway (RCP) experiments performed with 32 CMIP5 GCMs (see Table 1) to assess the ability of these experiments and their respective land surface models to reproduce the magnitude of the continental heat storage as estimated from borehole temperature measurements. The Historical experiment (1850–2005) [*van der Werf et al.*, 2006; *Schultz et al.*, 2008; *Mieville et al.*, 2010] is forced by observed atmospheric composition changes (natural and anthropogenic) and includes a time-dependent land cover representation [*Hurtt et al.*, 2011]. Additionally, some models (e.g., CANESM2 or GFDL-ESM2M) include dynamic vegetation to achieve a transient representation of the vegetation effect on the global climate. The RCP experiments [*van Vuuren et al.*, 2011b; *Meinshausen et al.*, 2011] are forced by greenhouse gas concentrations estimated from a range of emission and mitigation scenarios. RCPs take into account a series of socioeconomic changes and their impacts on emissions such as population growth or technological development from 2005 to 2100 and beyond. Four RCP experiments were used herein: RCP2.6 [*van Vuuren et al.*, 2011a], RCP4.5 [*Thomson et al.*, 2011], RCP6.0 [*Masui et al.*, 2011], and RCP8.5 [*Riahi et al.*, 2011]. We also use five of the available simulations for the Past1000 experiment [*Schmidt et al.*, 2012; *Braconnot et al.*, 2012] from the Paleoclimate Modeling Intercomparison Project Phase 3 (PMIP3), all of which are forced by reconstructed time-varying forcings from 850 to 1850 Common Era (C.E.).

2.2. Estimating GCM Subsurface Heat Storage

Previous studies have shown large differences in the simulated subsurface thermal regime in permafrost regions among the CMIP5 simulations, revealing the difficulties of the CMIP5 GCMs to simulate permafrost soils [*Koven et al.*, 2013; *Slater and Lawrence*, 2013]. We therefore limit calculations of the continental heat storage in each GCM simulation to the region between 60°N and 60°S, thus avoiding the high latitudes. The estimated continental heat storage from each GCM is then compared with the area-weighted estimates of heat storage in the continental landmasses obtained from a database of several hundred borehole temperature profiles distributed among six continents. These latter estimates range from 7×10^{21} J to 9×10^{21} J [*Beltrami et al.*, 2002; *Beltrami*, 2002; *Huang*, 2006] for all the continents except Antarctica from 1950 to 2000 C.E. If the observation-based results are restricted to the same 60°N–60°S domain adopted for the models, the area-weighted estimates range from 6×10^{21} J to 8×10^{21} J during the second half of the twentieth century.

Previous work [*DeGaetano et al.*, 1996; *Stevens et al.*, 2007] has estimated the heat storage from a simulated subsurface temperature anomaly according to

$$Q_s \propto \rho C \int_0^\infty T(z)\, dz, \tag{1}$$

where Q_s is the subsurface heat storage, ρC is the volumetric heat capacity of the ground, $T(z)$ is the subsurface temperature anomaly as a function of depth, and z is the depth. The heat capacity is considered constant at all depths in equation (1). The CMIP5 land surface models (LSMs) nevertheless estimate the heat capacity from a series of parameters dependent on time, depth, and geographic location. The heat integral therefore must

Table 1. CMIP5 Models Employed in This Paper[a]

Model	Land Surface Model	Number of Layers	Last Layer Depth	Last Node Depth	Land Model Reference
CCSM4	CLM4	15	43.74	35.18	*Oleson et al.* [2010]
CESM1-BGC	CLM4	15	43.74	35.18	*Oleson et al.* [2010]
CESM1-CAM5	CLM4	15	43.74	35.18	*Oleson et al.* [2010]
CESM1-FASTCHEM	CLM4	15	43.74	35.18	*Oleson et al.* [2010]
CESM1-WACCM	CLM4	15	43.74	35.18	*Oleson et al.* [2010]
NORESM1-M	CLM4	15	42.10	35.18	*Bentsen et al.* [2012]
NORESM1-ME	CLM4	15	42.10	35.18	*Bentsen et al.* [2012]
INM-CM4	INM-CM4	23	15.00	10.00	*Volodin et al.* [2010]
MIROC-ESM	MATSIRO	6	14.00	9.00	*Takata et al.* [2003]
MIROC-ESM-CHEM	MATSIRO	6	14.00	9.00	*Takata et al.* [2003]
MIROC5	MATSIRO	6	14.00	9.00	*Takata et al.* [2003]
GFDL-CM3	LM3	20	10.00	8.75	*Dunne et al.* [2012]
GFDL-ESM2G	LM3	20	10.00	8.75	*Dunne et al.* [2012]
GFDL-ESM2M	LM3	20	10.00	8.75	*Dunne et al.* [2012]
MRI-CGCM3	HAL	14	10.00	8.50	*Yukimoto et al.* [2012]
MRI-ESM1	HAL	14	10.00	8.50	*Yukimoto et al.* [2012]
MPI-ESM-LR	JSBACH	5	9.58	6.98	*Roeckner et al.* [2003]
MPI-ESM-MR	JSBACH	5	9.58	6.98	*Roeckner et al.* [2003]
MPI-ESM-P	JSBACH	5	9.58	6.98	*Roeckner et al.* [2003]
CMCC-CM	ECHAM5	5	6.98	4.83	*Roeckner et al.* [2003]
CMCC-CMS	ECHAM5	5	6.98	4.83	*Roeckner et al.* [2003]
CANESM2	CLASS2.7	3	4.10	2.23	*Verseghy* [1991]
IPSL-CM5A-LR	ORCHIDEE	7	3.86	3.86	*Krinner et al.* [2005]
IPSL-CM5A-MR	ORCHIDEE	7	3.86	3.86	*Krinner et al.* [2005]
PSL-CM5B-LR	ORCHIDEE	7	3.86	3.86	*Krinner et al.* [2005]
GISS-E2-R	GISS-LSM	6	3.50	2.73	*Rosenzweig and Abramopoulos* [1997]
GISS-E2-H	GISS-LSM	6	3.50	2.73	*Rosenzweig and Abramopoulos* [1997]
BCC-CSM1.1	BCC-AVIM1.0	10	3.43	2.86	*Wu et al.* [2014]
BCC-CSM1.1-M	BCC-AVIM1.0	10	3.43	2.86	*Wu et al.* [2014]
HADCM3	MOSES2	4	3.00	2.00	*Essery et al.* [2003]
HADGEM2-CC	MOSES2	4	3.00	2.00	*Essery et al.* [2003]
HADGEM2-ES	MOSES2	4	3.00	2.00	*Essery et al.* [2003]

[a]Each model is described by its land surface model, number of soil layers, bottom boundary placement (last node depth and last layer depth, in m) as well as the reference of its land surface model. All the land surface models use a zero-flux boundary condition at the bottom of the soil column.

be discretized for each grid cell following

$$Q_s = A \sum_{i=z_0}^{z_f} \rho C_i \cdot T_i \cdot \Delta z_i, \tag{2}$$

where Q_s is the subsurface heat storage (J), A is the area of the grid cell (m^2), and ρC_i, T_i, and Δz_i are the volumetric heat capacity (Jm^{-3}K^{-1}), the ground temperature (K), and the thickness (m) of the layer i, respectively. The direct application of equation (2) to each temperature profile is referred to as the LSM integration herein.

The volumetric heat capacity was estimated for each model following the theory of *van Wijk et al.* [1963] and the Community Land Model version 4 (CLM4) technical report [*Oleson et al.*, 2010]. We use this documentation because of its detailed description of thermal diffusion within a land surface model. The heat capacity depends on the type of soil, water, ice, and organic matter content at each grid cell and soil layer. Since the CMIP5 archive does not provide the composition of the soil layers in the simulations, the type of soil in each

grid cell, i.e., the percentage of sand and clay, was obtained from the ECOCLIMAP project [*Champeaux et al.*, 2005], an independent global database employed to initialize meteorological and climate models. Although it is probable that each CMIP5 simulation uses its own composition of sand and clay, the ECOCLIMAP database allows us to homogenize the estimates of continental heat storage among the 32 different CMIP5 GCMs. The organic matter fraction (f_{om}), defined as the ratio of the organic matter content at one soil layer to the maximum organic matter content that can be stored in one soil layer, was set as a parameter from the ground surface down to the depth of bedrock. Bedrock was imposed at 3.8 m depth for all the models that do not prescribe it to be consistent with the land surface model CLM4. Water and ice distributions in models without bedrock are unaltered. Thermal properties for bedrock are those from the CLM4 technical report. These arbitrary assumptions for the subsurface composition for each of the models were made because the CMIP5 archive does not provide these composition and thermal characteristics for each model. Our approach therefore homogenizes the estimates of heat storage in the continental subsurface among models, while adopting reasonable estimates for the physical quantities employed. Additionally, we derived estimates of the subsurface heat storage using only sand and clay compositions. Both soil configurations yielded similar results (not shown), thus we prescribed sand, clay and bedrock compositions in the estimates of continental heat storage presented in the Results and Discussion section to be consistent with the CLM4 documentation. Another approximation is related to the subsurface hydrology. The CMIP5 LSMs provide the water and ice content as a combined variable, which makes it impossible to separate the amount of water and ice in each soil layer. The ice content was thus considered as water content in this study. This approximation overestimates the volumetric heat capacity because of the larger specific heat capacity of the water ($c_{water}/c_{ice} \approx 2$). However, the effect of this approximation is considered negligible because our spatial domain avoids the majority of permafrost regions and therefore the majority of zones with perennial ground ice.

A forward model is used to assess how the depth of the bottom boundary condition in the land surface component of each GCM impacts estimates of the continental heat storage. The forward model is a purely conductive model for a semi-infinite and homogeneous half-space forced at the surface by a time-varying surface temperature function [*Carslaw and Jaeger*, 1959; *Beltrami and Mareschal*, 1992; *Beltrami et al.*, 1992; *Lesperance et al.*, 2010]. The forward model generates a subsurface temperature anomaly profile and is driven by the 1861–2000 surface air temperature (SAT) anomalies from each GCM simulation with initial conditions such that the temperature anomaly throughout the slab is 0 K. The resulting subsurface temperature profiles allow us to compare the effect of each GCM's simulated SAT on an identical subsurface volume, as well as provide estimates of the potential heat storage that GCMs could accumulate with a deeper bottom boundary. To complement the SAT-driven experiments, the forward model was also driven by the subsurface temperature anomaly at the bottom layer of each LSM, again to a depth of 500 m. The continental heat estimates from this extrapolation are then added to the result of the LSM integration, obtaining an additional estimate of the continental heat storage for the GCMs with an expanded bottom boundary. While this is an illustrative calculation, the estimate cannot substitute a climate simulation performed with a land surface model that explicitly employs a bottom boundary depth of 500 m because the bottom boundary can impact the thermal evolution of the subsurface above the depth of the boundary condition [*Smerdon and Stieglitz*, 2006]. An off-line simulation therefore only propagates the thermal state of the bottom boundary deeper into the subsurface, but it does not correctly incorporate the coupled impacts of near-surface soil processes that are unaffected by the location of a shallow bottom boundary.

3. Results and Discussion

The temporal evolution of the global multimodel mean soil temperature anomalies at a depth of 1.0 m for the Historical and RCP simulations (Figure 1a) are similar to the familiar trajectories of SAT for those simulations [*Hartmann et al.*, 2013]. This is also the case for the simulations extended for the past millennium (inset Figure 1a), suggesting a strong warming in the subsurface due to a changing climate forced by projected increases in CO_2 emissions relative to the historical and last millennium simulations. Nevertheless, the intermodel variability for the temporal evolution of these variables is large and depends on the RCP scenario. Globally, the largest warming and intermodel variability (2σ ensemble spread) are projected for the high latitudes of the northern hemisphere (Figures 1b and 1c) where simulated ground surface temperatures (GSTs) differ due to the presence of permafrost and associated active layer processes [*Koven et al.*, 2013; *Slater and Lawrence*, 2013].
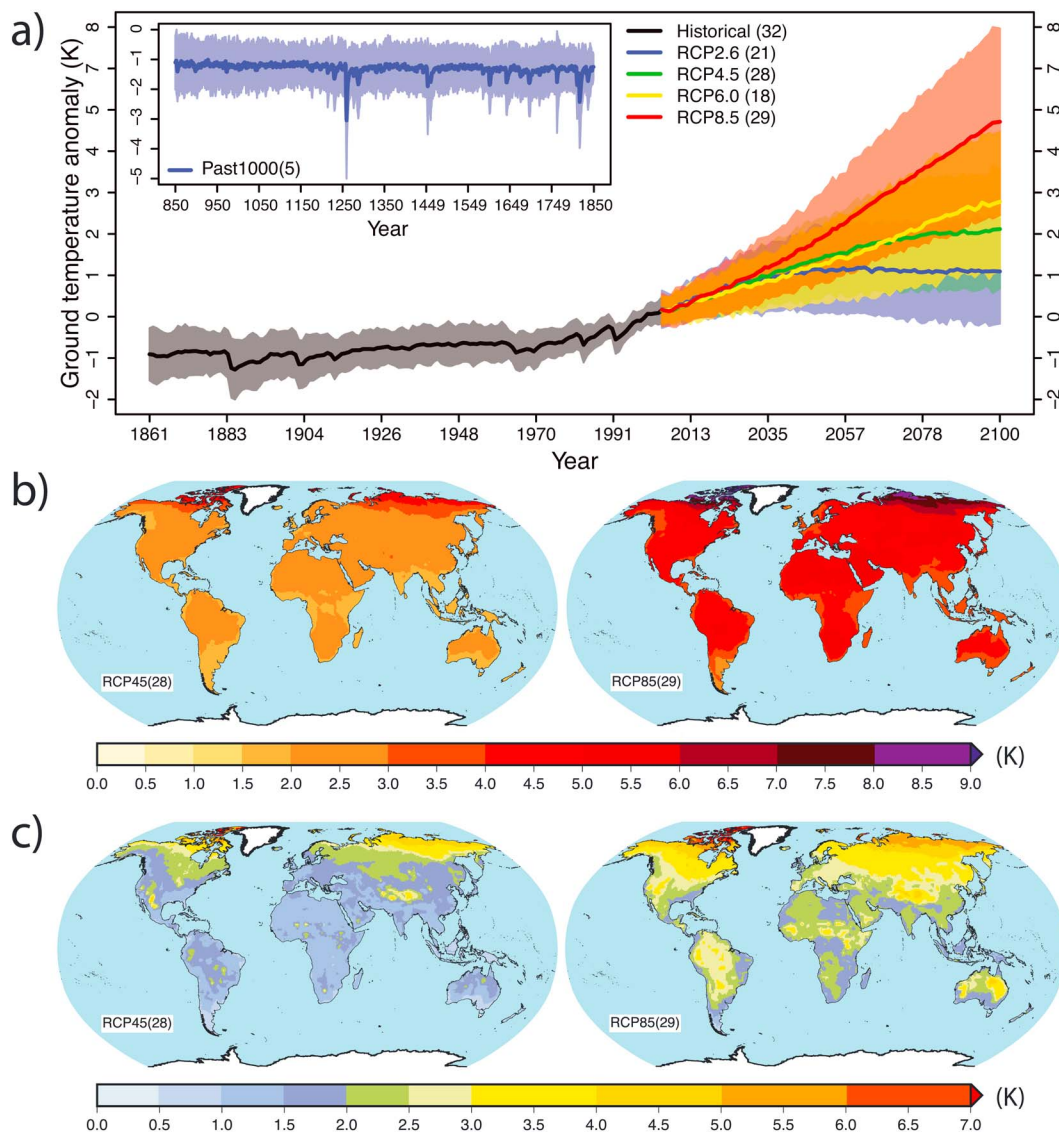
Figure 1. (a) Global mean soil temperature anomaly at 1.0 m depth relative to 1986–2005 [*Intergovernmental Panel on Climate Change (IPCC)*, 2013] determined by the CMIP5 ensemble of simulations. Lines represent the multimodel mean for each CMIP5 experiment. Shaded zones represent the 2σ ensemble spread. Each CMIP5 experiment is indicated by colors. Inset: global mean soil temperature anomaly at 1.0 m depth relative to 1986–2005 for the five PIMIP3 last millennium simulations. (b) Mean change in ground temperature and (c) 2σ range based in multimodel mean projections for 2081–2100 relative to 1986–2005 [*IPCC*, 2013] at 1.0 m of depth. Figures 1b (left) and 1c (left) show results for RCP4.5 pathway. Figures 1b (right) and 1c (right) show results for RCP8.5 pathway. Results for RCP2.6 and RCP6.0 are shown in the supporting information (Figure S1). The number of models used in the calculations is indicated in parenthesis.

Because the heat is estimated from the integration of the subsurface temperature profiles, the warming of the GSTs and subsequent propagation of the warming into the subsurface during the second half of the twentieth century should generate a net gain of heat in the continental subsurface in both the simulations and observed estimates from borehole profiles. The integration of the simulated subsurface temperatures (equation (2)) from the 32 CMIP5 GCMs, however, yields a smaller estimate of the continental heat storage on average (Figures 2a, red bars and 2b, crosses) between 1950 and 2000 than that inferred from geothermal data [*Beltrami*, 2002; *Beltrami et al.*, 2002] and, indirectly, from meteorological data [*Huang*, 2006]. Additionally, six of the models yield negative values for the subsurface heat storage, indicating a continental energy loss for the same time period. These results are unsupported by geothermal data. The multimodel mean and ensemble spread (2σ) are $1 \pm 5 \times 10^{21}$ J, while the geothermal range is $\sim 7 \pm 1 \times 10^{21}$ J. One explanation for
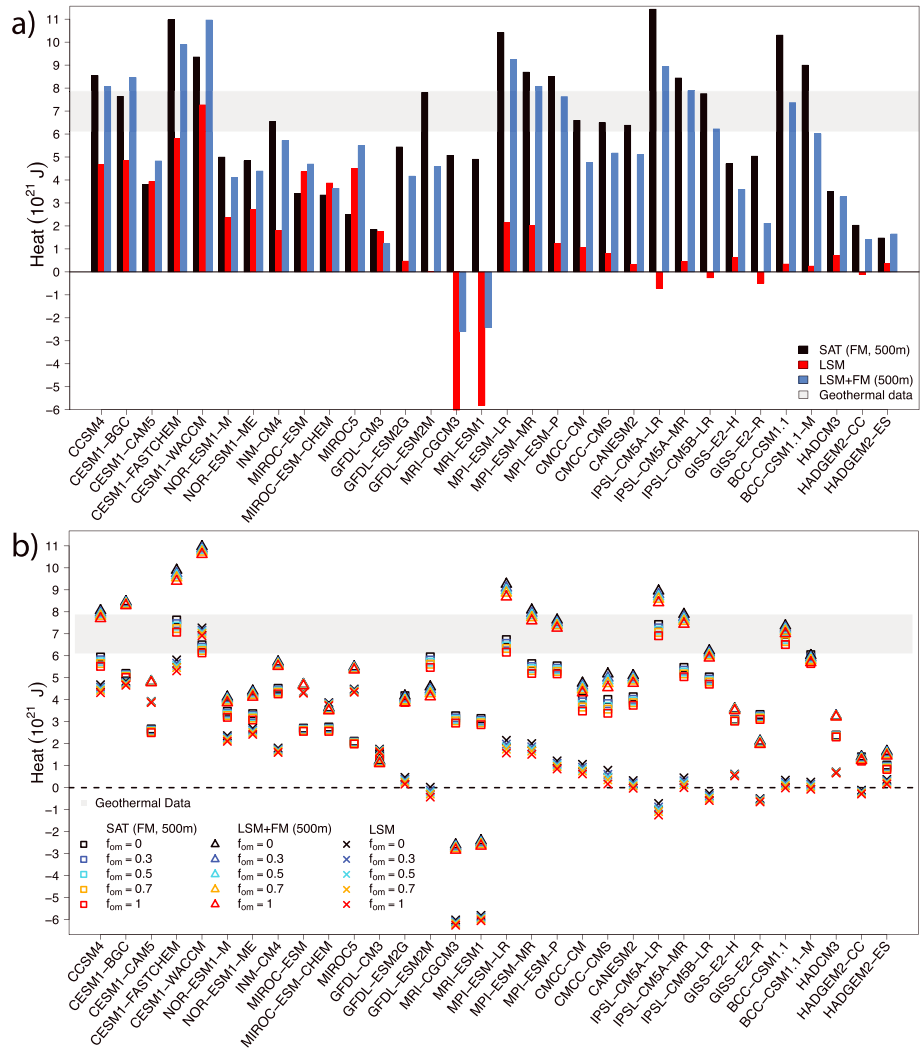
Figure 2. (a) Continental heat storage for the domain bounded by 60°N–60°S from the period 1950–2000. Red bars represent the magnitudes of heat storage directly from the land surface model integrations (see equation (2)). In black, results using the forward model (constant $\rho C = 3.0 \times 10^6 \, \mathrm{J \, m^{-3} K^{-1}}$) and SAT anomaly relative to 1861–2000 as the surface forcing and a bottom boundary depth of 500 m. Blue bars represent the heat storage from the forward model of subsurface temperatures to 500 m plus the estimated heat storage from the direct integration of each model (red bars). (b) Continental heat storage taking into account different values of the organic matter fraction (f_{om}). Crosses represent the estimated heat storage from the land surface model integration (equation (2)). Squares represent continental heat storage using the forward model and SAT anomaly relative to 1861–2000 as upper forcing and bottom boundary depth at 500 m. The heat storage was estimated taking into account the estimated volumetric heat capacity for each model and considering $\rho C = 3.0 \times 10^6 \mathrm{Jm^{-3}K^{-1}}$ beyond the bottom boundary depth. Triangles represent the estimated heat storage from the forward model of subsurface temperatures to 500 m plus the estimated heat storage from the direct integration of each model (crosses). Grey band in both panels represent the range of continental heat storage from borehole temperature data scaled to the domain considered here ($7 \pm 1 \times 10^{21}$ J) [*Beltrami*, 2002; *Beltrami et al.*, 2002]. Models are listed from the deepest to the shallowest bottom boundary depth.

the discrepancy between the estimated continental heat gain and the modeled heat gains is the depth to which the continental subsurface is modeled in the GCMs [*Stevens et al.*, 2007; *MacDougall et al.*, 2008, 2010]. The shallow depth of the bottom boundaries in most models places a physical limit on the volume of the continental subsurface that is available for storing heat.

In order to test the impact of the bottom boundary depth in the CMIP5 land surface models, we use the forward model to simulate the subsurface temperature evolution using changes in SAT and GST from the GCM simulations and allowing heat to diffuse to a depth of 500 m. The magnitude of the continental energy storage obtained in this fashion (Figure 2a, black bars and blue bars) is in better agreement with those estimates from
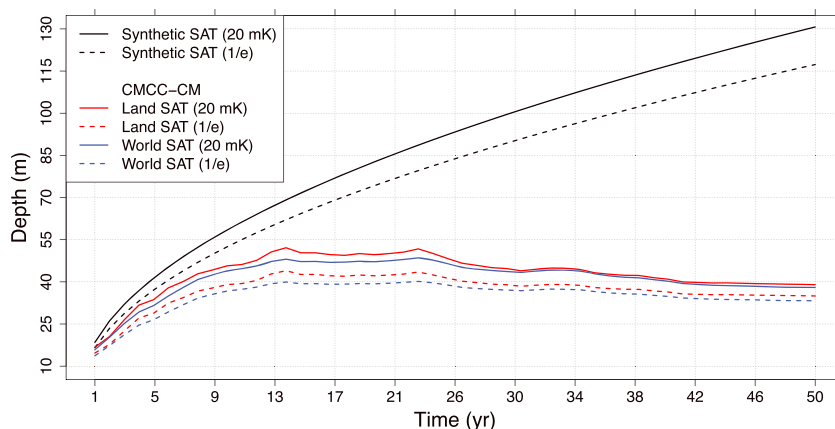
Figure 3. Depth required to record a surface temperature contribution to the subsurface heat storage during different time intervals. In black, results use a synthetic signal that consists of a 1 K change beginning t years ago, where t is the duration of the signal. In red, results using the mean SAT anomaly from Centro Euro-Mediterraneo sui Cambiamenti Climatici-Climate Model (CMCC-CM) over landmasses, and in blue results using the global SAT anomaly from the CMCC-CM model. The criterion of convergence is indicated in brackets.

geothermal data for the same time period ($6 \pm 6 \times 10^{21}$ J). This improvement on the estimates of continental heat storage from CMIP5 GCM simulations reinforces the idea that the limitation of the available continental volume to store energy, imposed by the shallow depth of the CMIP5 land surface components, is the main physical reason for the differences between CMIP5 simulations and geothermal estimates as discussed above.

For completeness, the continental heat storage was also estimated for a range of soil organic matter fractions (f_{om}) (Figure 2b), reaching similar results for all f_{om} values from $f_{om} = 0$ to $f_{om} = 1$. Higher values of f_{om} lead to lower values of continental heat storage, but the difference between using $f_{om} = 0$ or $f_{om} = 1$ is not a determinant factor and does not improve the discrepancies between the estimated continental heat storage from the CMIP5 simulations and the geophysical estimates.

The restriction placed by the depth of the bottom boundary on the available volume for subsurface heat storage also implies a constraint on the temporal interval of the evolution of the surface energy imbalance that is predominantly recorded in the subsurface. That is, the ground loses the signal or "memory" of the climate system changes over different times depending on the lower boundary depth—in the case of CMIP5 simulations with CLM4, this time is no longer than a few decades [see *Stevens et al.*, 2007; *Smerdon and Stieglitz*, 2006] (Figure 3). To assess the effect of the limited depth of the land surface component on the heat content, we used the forward model forced by (1) a synthetic 1 K step change in ground surface temperature (GST) occurring from one to fifty years before present and (2) a time-varying upper boundary condition from a simulation of global and continental SAT anomalies from one of the CMIP5 GCMs that is selected as an arbitrary example, namely, the Centro Euro-Mediterraneo sui Cambiamenti Climatici-Climate Model (CMCC-CM).

As expected, the depth reached by the temperature variation increases with time. The synthetic temperature variation (Figure 3, black lines) reaches 130 m after 50 years using the typical measurement error in borehole temperature profiles (20 mK) as the criterion of convergence. The thermal effect reaches 117 m in the same period using the skin depth (e^{-1} K) as the criterion of convergence [*Stevens et al.*, 2007]. Therefore, none of the 32 CMIP5 GCMs has a land component deep enough to record the temperature profile produced by 50 years of the synthetic experiment. Perhaps more realistically, the results of the global and the continental SAT anomalies from the CMCC-CM (Figure 3, blue and red lines) suggest that only the models with a bottom boundary deeper than 34 m may record the surface temperature variations and their contributions to the subsurface thermal regime between 1950 and 2000, according to both depth criteria. Considering these results, all GCMs using the CLM4 as their land surface component (and the associated bottom boundary depth) should be able to reproduce a continental heat content close to the estimate obtained from geothermal data. However, our results show that only the Community Earth System Model version one-Whole Atmosphere Community Climate Model (CESM1-WACCM) yields subsurface heat content within the range of those obtained from data (Figures 2a and 2b), despite there being other models that are deeper than 40 m (see Table 1). This discrepancy may be the result of the differences in the parameterization of the energy exchange processes at the

air-ground interface and the coupling between each atmospheric model and the CLM4 land surface component, as well as the different sensitivities (equilibrium climate sensitivity and transient climate response) of each GCM to the external forcing [*Andrews et al.*, 2012; *Forster et al.*, 2013]. It is also possible that the maximum depth reached by the surface air temperature variations for this 50 year period is larger than the CLM4 bottom boundary depth, thus losing some thermal information.

Although the effect of the shallow bottom boundary placement and the SAT of each GCM simulation can offer an explanation for the discrepancies between GCM estimates of continental heat storage and those retrieved from borehole temperature data in the period 1950–2000, the negative magnitude of subsurface heat storage estimated for both Meteorological Research Institute (MRI) models cannot be explained by the above arguments. For both of these models, the water and ice content in the ground (mrso variable in the CMIP5 archive) presents a marked negative trend for the Historical experiment, which affects our continental energy storage estimates. However, both MRI GCMs simulate a subsurface temperature increase for the same experiment, suggesting a decoupling between the simulation of heat diffusion and surface and subsurface hydrology. Indeed, if we ignore the hydrology and the associated removal of energy from the subsurface by runoff and infiltration, then both MRI GCMs yield positive continental energy storage values, indicating that the marked decrease in the ground water content in the MRI simulations is responsible for their negative continental heat storage estimates (Figures 2a and 2b).

4. Conclusions

This is the first work to examine ground temperature trajectories and associated estimates of subsurface heat content from the CMIP5 simulation archive. We have found that the temporal evolution of the simulated ground temperature exhibits similar warming trends and temporal variability ranges as that reported for surface air temperature in the Historical and RCP CMIP5 experiments [*IPCC*, 2013]. This clearly indicates a first order thermal coupling between the lower atmosphere and the ground, in agreement with the analysis of *García-García et al.* [2016, ERL] for the five CMIP5/PMIP3 last millennium simulations used herein.

The majority of CMIP5 GCMs show a net heat gain in the subsurface for the second half of the twentieth century, as expected due to the warming of the ground surface during this period. However, only one GCM simulation yields a heat storage estimate for the 1950–2000 period that is comparable to the quantity estimated from geothermal data. The multimodel mean and ensemble spread (2σ) in the simulated continental heat storage are $1 \pm 5 \times 10^{21}$ J, while the geophysical data estimate a value of $7 \pm 1 \times 10^{21}$ J.

The smaller magnitude of estimated subsurface energy storage from the CMIP5-GCM simulations is mainly due to the limited thermal memory imposed by the depth of the bottom boundary in the land surface components of the CMIP5 GCMs. That is, the thermal contribution from the surface energy imbalance cannot be physically recorded underground for more than 1 or 2 years for 27 of 32 CMIP5 GCMs, due to the fact that the bottom boundary placement in their land surface models is shallower than 16 m. When we allow the propagation of heat to 500 m using the forward model, the magnitude of each model simulation's subsurface heat content are in better agreement with the geothermal measurements. These estimates of continental heat storage nevertheless display a large range of variability. Although the different bottom boundary depths of the GCM land surface components account for most of this variability, further work is needed to address and clarify the effects of other possible sources of variability on the estimates of continental heat storage from GCM simulations. Nevertheless, despite these possible minor sources of variability, the principal disagreement between the GCM and observation-based estimates of heat storage in the continental subsurface reflects the fact that the current generation of GCMs does not represent well the continental component of heat storage in the Earth's energy budget. As a simplistic estimate of the variation in the ground temperature dictated by the lack of subsurface energy in the CMIP5 GCMs, we calculate the mean change of the subsurface temperature for the period 1950–2000 C.E. in our spatial domain from the CESM1-WACCM GCM simulation. This GCM simulation yielded a continental heat storage with similar magnitude to the difference between geothermal estimates and the multimodel mean of subsurface energy change from the CMIP5 ensemble. Such change in subsurface energy storage achieves a temperature increase of 0.67 K at 2.8 m. Although this estimate depends on several factors including the latitude or depth, such mean temperature change is not negligible due to its possible effect on surface and near-surface processes. Future model refinements should therefore work to

implement deeper bottom boundaries in land surface models, improving the ability of GCMs to represent the subsurface energy content and thus enhancing the representation of near-surface processes with potentially important climate feedbacks such as the stability and evolution of soil carbon and permafrost.

References

Alexeev, V. A., D. J. Nicolsky, V. E. Romanovsky, and D. M. Lawrence (2007), An evaluation of deep soil configurations in the CLM3 for improved representation of permafrost, *Geophys. Res. Lett.*, *34*, L09502, doi:10.1029/2007GL029536.

Andrews, T., J. M. Gregory, M. J. Webb, and K. E. Taylor (2012), Forcing, feedbacks and climate sensitivity in CMIP5 coupled atmosphere-ocean climate models, *Geophys. Res. Lett.*, *39*, L09712, doi:10.1029/2012GL051607.

Arora, V. K., et al. (2013), Carbon–concentration and carbon–climate feedbacks in CMIP5 earth system models, *J. Clim.*, *26*(15), 5289–5314, doi:10.1175/JCLI-D-12-00494.1.

Beltrami, H. (2002), Climate from borehole data: Energy fluxes and temperatures since 1500, *Geophys. Res. Lett.*, *29*(23), 2111, doi:10.1029/2002GL015702.

Beltrami, H., and J.-C. Mareschal (1992), Ground temperature histories for central and eastern Canada from geothermal measurements: Little ice age signature, *Geophys. Res. Lett.*, *19*(7), 689–692, doi:10.1029/92GL00671.

Beltrami, H., A. M. Jessop, and J.-C. Mareschal (1992), Ground temperature histories in eastern and central canada from geothermal measurements: Evidence of climatic change, *Global Planet. Change*, *6*(2–4), 167–183, doi:10.1016/0921-8181(92)90033-7.

Beltrami, H., J. E. Smerdon, H. N. Pollack, and S. Huang (2002), Continental heat gain in the global climate system, *Geophys. Res. Lett.*, *29*(8), 8–1–8–3, doi:10.1029/2001GL014310.

Bentsen, M., et al. (2012), The Norwegian Earth System Model, NorESM1-M—Part 1: Description and basic evaluation, *Geosci. Model Dev. Discuss.*, *5*(3), 2843–2931, doi:10.5194/gmdd-5-2843-2012.

Braconnot, P., S. P. Harrison, M. Kageyama, P. J. Bartlein, V. Masson-Delmotte, A. Abe-Ouchi, B. Otto-Bliesner, and Y. Zhao (2012), Evaluation of climate models using palaeoclimatic data, *Nat. Clim. Change*, *2*(6), 417–424.

Carslaw, H., and J. Jaeger (1959), *Conduction of Heat in Solids*, Clarendon Press, Oxford.

Champeaux, J. L., V. Masson, and F. Chauvin (2005), Ecoclimap: A global database of land surface parameters at 1 km resolution, *Meteorol. Appl.*, *12*(1), 29–32, doi:10.1017/S1350482705001519.

DeGaetano, A. T., D. S. Wilks, and M. McKay (1996), A physically based model of soil freezing in humid climates using air temperature and snow cover data, *J. Appl. Meteorol.*, *35*(6), 1009–1027, doi:10.1175/1520-0450(1996)035<1009:APBMOS>2.0.CO;2.

Dunne, J. P., et al. (2012), Gfdl's ESM2 global coupled climate–carbon earth system models. Part I: Physical formulation and baseline simulation characteristics, *J. Clim.*, *25*(19), 6646–6665, doi:10.1175/JCLI-D-11-00560.1.

Essery, R. L. H., M. J. Best, R. A. Betts, P. M. Cox, and C. M. Taylor (2003), Explicit representation of subgrid heterogeneity in a GCM land surface scheme, *J. Hydrometeorol.*, *4*(3), 530–543, doi:10.1175/1525-7541(2003)004<0530:EROSHI>2.0.CO;2.

Forster, P. M., T. Andrews, P. Good, J. M. Gregory, L. S. Jackson, and M. Zelinka (2013), Evaluating adjusted forcing and model spread for historical and future scenarios in the CMIP5 generation of climate models, *J. Geophys. Res. Atmos.*, *118*, 1139–1150, doi:10.1002/jgrd.50174.

Friedlingstein, P., et al. (2006), Climate–carbon cycle feedback analysis: Results from the C4MIP model intercomparison, *J. Clim.*, *19*(14), 3337–3353, doi:10.1175/JCLI3800.1.

García-García A., F. J. Cuesta-Valero, H. Beltrami, and J. E. Smerdon (2016), Simulation of air and ground temperatures in PIMIP3/CMIP5 last millennium simulation: Implications for climate reconstructions from borehole temperature profiles, *Environ. Res. Lett.*, *11*(4), 044022, doi:10.1088/1748-9326/11/4/044022.

González-Rouco, J. F., H. Beltrami, E. Zorita, and M. B. Stevens (2009), Borehole climatology: A discussion based on contributions from climate modeling, *Clim. Past*, *5*(1), 97–127, doi:10.5194/cp-5-97-2009.

Hansen, J., M. Sato, P. Kharecha, and K. V. Schuckmann (2011), Earth's energy imbalance and implications, *Atmos. Chem. Phys.*, *11*(24), 13,421–13,449.

Hartmann, D., et al. (2013), Observations: Atmosphere and surface, in *Climate Change 2013: The Physical Science Basis. Contribution of Working Group I to the Fifth Assessment Report of the Intergovernmental Panel on Climate Change*, book section, vol. 2, edited by T. Stocker et al., pp. 159–254, Cambridge Univ. Press, Cambridge, U. K., and New York, doi:10.1017/CBO9781107415324.008.

Hicks Pries, C. E., E. A. G. Schuur, S. M. Natali, and K. G. Crummer (2016), Old soil carbon losses increase with ecosystem respiration in experimentally thawed tundra, *Nat. Clim. Change*, *6*(2), 214–218.

Huang, S. (2006), 1851–2004 annual heat budget of the continental landmasses, *Geophys. Res. Lett.*, *33*, L04707, doi:10.1029/2005GL025300.

Hurtt, G., et al. (2011), Harmonization of land-use scenarios for the period 1500–2100: 600 years of global gridded annual land-use transitions, wood harvest, and resulting secondary lands, *Clim. Change*, *109*(1–2), 117–161, doi:10.1007/s10584-011-0153-2.

Intergovernmental Panel on Climate Change (IPCC) (2013), *Climate Change 2013: The Physical Science Basis. Contribution of Working Group I to the Fifth Assessment Report of the Intergovernmental Panel on Climate Change*, p. 1535, Cambridge Univ. Press, Cambridge, U. K., and New York.

Koven, C. D., W. J. Riley, and A. Stern (2013), Analysis of permafrost thermal dynamics and response to climate change in the CMIP5 Earth System Models, *J. Clim.*, *26*(6), 1877–1900, doi:10.1175/JCLI-D-12-00228.1.

Krakauer, N. Y., M. J. Puma, and B. I. Cook (2013), Impacts of soil–aquifer heat and water fluxes on simulated global climate, *Hydrol. Earth Syst. Sci.*, *17*(5), 1963–1974, doi:10.5194/hess-17-1963-2013.

Krinner, G., N. Viovy, N. de Noblet-Ducoudré, J. Ogée, J. Polcher, P. Friedlingstein, P. Ciais, S. Sitch, and I. C. Prentice (2005), A dynamic global vegetation model for studies of the coupled atmosphere-biosphere system, *Global Biogeochem. Cycles*, *19*(1), GB1015, doi:10.1029/2003GB002199.

Lawrence, D. M., A. G. Slater, V. E. Romanovsky, and D. J. Nicolsky (2008), Sensitivity of a model projection of near-surface permafrost degradation to soil column depth and representation of soil organic matter, *J. Geophys. Res.*, *113*, F02011, doi:10.1029/2007JF000883.

Lesperance, M., J. E. Smerdon, and H. Beltrami (2010), Propagation of linear surface air temperature trends into the terrestrial subsurface, *J. Geophys. Res.*, *115*, D21115, doi:10.1029/2010JD014377.

Levitus, S., J. Antonov, and T. Boyer (2005), Warming of the world ocean, 1955–2003, *Geophys. Res. Lett.*, *32*, L02604, doi:10.1029/2004GL021592.

Levitus, S., J. I. Antonov, T. P. Boyer, R. A. Locarnini, H. E. Garcia, and A. V. Mishonov (2009), Global ocean heat content 1955–2008 in light of recently revealed instrumentation problems, *Geophys. Res. Lett.*, *36*, L07608, doi:10.1029/2008GL037155.

MacDougall, A. H., J. F. González-Rouco, M. B. Stevens, and H. Beltrami (2008), Quantification of subsurface heat storage in a GCM simulation, *Geophys. Res. Lett.*, *35*, L13702, doi:10.1029/2008GL034639.

MacDougall, A. H., H. Beltrami, J. F. González-Rouco, M. B. Stevens, and E. Bourlon (2010), Comparison of observed and general circulation model derived continental subsurface heat flux in the Northern Hemisphere, *J. Geophys. Res.*, *115*, D12109, doi:10.1029/2009JD013170.

Masui, T., et al. (2011), An emission pathway for stabilization at 6 Wm^{-2} radiative forcing, *Clim. Change*, *109*(1–2), 59–76, doi:10.1007/s10584-011-0150-5.

Meinshausen, M., et al. (2011), The RCP greenhouse gas concentrations and their extensions from 1765 to 2300, *Clim. Change*, *109*(1–2), 213–241, doi:10.1007/s10584-011-0156-z.

Mieville, A., C. Granier, C. Liousse, B. Guillaume, F. Mouillot, J.-F. Lamarque, J.-M. Grégoire, and G. Pétron (2010), Emissions of gases and particles from biomass burning during the 20th century using satellite data and an historical reconstruction, *Atmos. Environ.*, *44*(11), 1469–1477, doi:10.1016/j.atmosenv.2010.01.011.

Nicolsky, D. J., V. E. Romanovsky, V. A. Alexeev, and D. M. Lawrence (2007), Improved modeling of permafrost dynamics in a GCM land-surface scheme, *Geophys. Res. Lett.*, *34*, L08501, doi:10.1029/2007GL029525.

Oelke, C., and T. Zhang (2004), A model study of circum-Arctic soil temperatures, *Permafrost and Periglacial Processes*, *15*(2), 103–121, doi:10.1002/ppp.485.

Oleson, K. W., et al. (2010), Technical description of version 4.0 of the Community Land Model (CLM), *Tech. Rep., NCAR Tech. Note NCAR/TN-478+STR*, Natl. Cent. for Atmos. Res., Boulder, Colo.

Pollack, H. N., J. E. Smerdon, and P. E. van Keken (2005), Variable seasonal coupling between air and ground temperatures: A simple representation in terms of subsurface thermal diffusivity, *Geophys. Res. Lett.*, *32*, L15405, doi:10.1029/2005GL023869.

Pollard, D., R. M. DeConto, and A. A. Nyblade (2005), Sensitivity of Cenozoic Antarctic Ice Sheet variations to geothermal heat flux, *Global Planet. Change*, *49*(1–2), 63–74, doi:10.1016/j.gloplacha.2005.05.003.

Riahi, K., S. Rao, V. Krey, C. Cho, V. Chirkov, G. Fischer, G. Kindermann, N. Nakicenovic, and P. Rafaj (2011), RCP 8.5 — A scenario of comparatively high greenhouse gas emissions, *Clim. Change*, *109*(1–2), 33–57, doi:10.1007/s10584-011-0149-y.

Roeckner, E., et al. (2003), Model description of the atmospheric general circulation model ECHAM5. Part I: Model description, *Tech. Rep. MPI-Report No. 349*, p. 127, Max-Planck-Institut für Meteorologie, Hamburg, Germany.

Rosenzweig, C., and F. Abramopoulos (1997), Land-surface model development for the GISS GCM, *J. Clim.*, *10*(8), 2040–2054, doi:10.1175/1520-0442(1997)010<2040:LSMDFT>2.0.CO;2.

Schmidt, G. A., et al. (2012), Climate forcing reconstructions for use in PMIP simulations of the last millennium (v1.1), *Geosci. Model Dev.*, *5*(1), 185–191, doi:10.5194/gmd-5-185-2012.

Schultz, M. G., A. Heil, J. J. Hoelzemann, A. Spessa, K. Thonicke, J. G. Goldammer, A. C. Held, J. M. C. Pereira, and M. van het Bolscher (2008), Global wildland fire emissions from 1960 to 2000, *Global Biogeochem. Cycles*, *22*(2), GB2002, doi:10.1029/2007GB003031.

Sitch, S., et al. (2008), Evaluation of the terrestrial carbon cycle, future plant geography and climate-carbon cycle feedbacks using five dynamic global vegetation models (DGVMS), *Global Change Biol.*, *14*(9), 2015–2039, doi:10.1111/j.1365-2486.2008.01626.x.

Slater, A. G., and D. M. Lawrence (2013), Diagnosing present and future permafrost from climate models, *J. Clim.*, *26*(15), 5608–5623, doi:10.1175/JCLI-D-12-00341.1.

Smerdon, J. E., and M. Stieglitz (2006), Simulating heat transport of harmonic temperature signals in the Earth's shallow subsurface: Lower-boundary sensitivities, *Geophys. Res. Lett.*, *33*, L14402.

Stevens, M. B., J. E. Smerdon, J. F. González-Rouco, M. Stieglitz, and H. Beltrami (2007), Effects of bottom boundary placement on subsurface heat storage: Implications for climate model simulations, *Geophys. Res. Lett.*, *34*, L02702, doi:10.1029/2006GL028546.

Stieglitz, M., and J. E. Smerdon (2007), Characterizing land–atmosphere coupling and the implications for subsurface thermodynamics, *J. Clim.*, *20*(1), 21–37, doi:10.1175/JCLI3982.1.

Takata, K., S. Emori, and T. Watanabe (2003), Development of the minimal advanced treatments of surface interaction and runoff, *Global Planet. Change*, *38*(1–2), 209–222, doi:10.1016/S0921-8181(03)00030-4.

Tarnocai, C., J. G. Canadell, E. A. G. Schuur, P. Kuhry, G. Mazhitova, and S. Zimov (2009), Soil organic carbon pools in the northern circumpolar permafrost region, *Global Biogeochem. Cycles*, *23*(2), GB2023, doi:10.1029/2008GB003327.

Taylor, K. E., R. J. Stouffer, and G. A. Meehl (2011), An overview of CMIP5 and the experiment design, *Bull. Am. Meteorol. Soc.*, *93*(4), 485–498, doi:10.1175/BAMS-D-11-00094.1.

Thomson, A., et al. (2011), RCP4.5: A pathway for stabilization of radiative forcing by 2100, *Clim. Change*, *109*(1–2), 77–94, doi:10.1007/s10584-011-0151-4.

van der Werf, G. R., J. T. Randerson, L. Giglio, G. J. Collatz, P. S. Kasibhatla, and A. F. Arellano Jr. (2006), Interannual variability in global biomass burning emissions from 1997 to 2004, *Atmos. Chem. Phys.*, *6*(11), 3423–3441, doi:10.5194/acp-6-3423-2006.

van Vuuren, D., et al. (2011a), RCP2.6: Exploring the possibility to keep global mean temperature increase below 2°C, *Clim. Change*, *109*(1–2), 95–116, doi:10.1007/s10584-011-0152-3.

van Vuuren, D., et al. (2011b), The representative concentration pathways: An overview, *Clim. Change*, *109*(1–2), 5–31, doi:10.1007/s10584-011-0148-z.

van Wijk, W. R., A. J. W. Borghrst, J. A. Businger, W. J. Derksen, F. H. Schmidt, D. W. Scholte Ubing, and D. A. de Vries (1963), *Physics Plant Environmnet*, North-Holland Comp., Amsterdam.

Verseghy, D. L. (1991), Class — A Canadian land surface scheme for GCMS. I. Soil model, *Int. J. Climatol.*, *11*(2), 111–133, doi:10.1002/joc.3370110202.

Volodin, E., N. Dianskii, and A. Gusev (2010), Simulating present-day climate with the INMCM4.0 coupled model of the atmospheric and oceanic general circulations, *Izvestiya Atmos. Ocean Phys.*, *46*(4), 414–431, doi:10.1134/S000143381004002X.

Weidong, G., S. Shufen, and Q. Yongfu (2002), Case analyses and numerical simulation of soil thermal impacts on land surface energy budget based on an off-line land surface model, *Adv. Atmos. Sci.*, *19*(3), 500–512, doi:10.1007/s00376-002-0082-0.

Wu, T., et al. (2014), An overview of bcc climate system model development and application for climate change studies, *J. Meteorol. Res.*, *28*(1), 34–56, doi:10.1007/s13351-014-3041-7.

Yukimoto, S., et al. (2012), A new global climate model of the Meteorological Research Institute: MRI-CGCM3 – model description and basic performance, *J. Meteorol. Soc. Jpn. Ser. II*, *90A*, 23–64, doi:10.2151/jmsj.2012-A02.